


# Evaluation of Cadmium-Zinc-Telluride Detector-based Single-Photon Emission Computed Tomography for Nuclear Cardiology: a Comparison with Conventional Anger Single-Photon Emission Computed Tomography

Takanaga Niimi<sup>1</sup>  · Mamoru Nanasato<sup>2</sup> · Mitsuo Sugimoto<sup>1</sup> · Hisatoshi Maeda<sup>3</sup>

Received: 13 September 2016 / Revised: 5 December 2016 / Accepted: 30 January 2017 / Published online: 3 March 2017  
© Korean Society of Nuclear Medicine 2017

## Abstract

**Purpose** The differences in performance between the cadmium-zinc-telluride (CZT) camera or collimation systems and conventional Anger single-photon emission computed tomography (A-SPECT) remain insufficient from the viewpoint of the user. We evaluated the performance of the D-SPECT (Spectrum Dynamics, Israel) system to provide more information to the cardiologist or radiological technologist about its use in the clinical field.

**Materials and Methods** This study evaluated the performance of the D-SPECT system in terms of energy resolution, detector sensitivity, spatial resolution, modulation transfer function (MTF), and collimator resolution in comparison with that of A-SPECT (Bright-View, Philips, Japan). Energy resolution and detector sensitivity were measured for Tc-99m, I-123, and Tl-201. The SPECT images produced by both systems were evaluated visually using the anthropomorphic torso phantom.

**Results** The energy resolution of D-SPECT with Tc-99m and I-123 was approximately two times higher than that of A-SPECT. The detector sensitivity of D-SPECT was higher than that of A-SPECT (Tc-99m: 4.2 times, I-123: 2.2 times, and Tl-

201: 5.9 times). The mean spatial resolution of D-SPECT was two times higher than that of A-SPECT. The MTF of D-SPECT was superior to that of the A-SPECT system for all frequencies. The collimator resolution of D-SPECT was lower than that of A-SPECT; however, the D-SPECT images clearly indicated better spatial resolution than the A-SPECT images. **Conclusion** The energy resolution, detector sensitivity, spatial resolution, and MTF of D-SPECT were superior to those of A-SPECT. Although the collimator resolution was lower than that of A-SPECT, the D-SPECT images were clearly of better quality.

**Keywords** Anger SPECT · Collimation system · CZT camera · D-SPECT · Nuclear cardiology

## Introduction

Over the last few decades, the quality of images acquired from medical imaging techniques such as single-photon emission computerized tomography (SPECT) and positron emission tomography has improved because of advances in material sciences and information technologies [1]. Remarkable progress has been made in the spatial and energy resolutions of SPECT images, making it possible to detect a defect less than a few millimeters in diameter [2–4]. Recently, cardiac SPECT systems equipped with cadmium-zinc-telluride (CZT) detectors have been introduced into clinical practice [5–7]. This new technology provides a higher speed and resolution than NaI scintillation detectors, which are used in conventional Anger cameras, and has the potential to revolutionize nuclear cardiology [8–10]. High-speed SPECT systems with CZT detectors (D-SPECT, Spectrum Dynamics, Israel) have been recently introduced and exhibit both high-sensitivity

✉ Takanaga Niimi  
nim@nagoya2.jrc.or.jp

<sup>1</sup> Department of Radiological Technology, Nagoya Daini Red Cross Hospital, Takanaga Niimi, 2-9 Myouken-cho, Showa-ku, Nagoya 466-8650, Japan  
<sup>2</sup> Cardiovascular Center, Nagoya Daini Red Cross Hospital, 2-9 Myouken-cho, Showa-ku, Nagoya 466-8650, Japan  
<sup>3</sup> Department of Radiological Technology, Nagoya University School of Health Sciences, 1-1-20 Daiko-minami, Higashi-ku, Nagoya 461-8673, Japan

collimation and high-energy resolution for cardiac imaging [8–10]. Compared with conventional systems, the D-SPECT system is unique because it has no external moving parts; it rests closer to the patient's chest during imaging, and imaging is performed with the patient in an upright position, and with their arms over the detectors (versus arms raised over their head) [11]. Therefore, this cardiac imaging technique is comfortable for the patient and may reduce motion artifacts [12–14]. However, although some research organizations have compared the performance of the CZT camera and collimation systems with that of conventional and new systems [8–10], the differences remain insufficient from the viewpoint of the user, such as multiple tracers or the influence of detector-tracer distance on image qualities, and so on. In this study, we evaluated the performance of CZT cameras and collimation systems in the D-SPECT system and compared the results with those of a conventional Anger SPECT (A-SPECT) system.

## Materials and Methods

### SPECT System

We compared the performance of the D-SPECT system with that of a conventional A-SPECT system in terms of energy resolution, detector sensitivity, spatial resolution, modulation transfer function (MTF), and collimator resolution. The semiconductor in the D-SPECT system is equipped with nine CZT detector arrays, and each detector block consists of  $16 \times 64$  individual pixels with a spacing of 2.46 mm in both dimensions resulting in a total detector surface of  $39.4 \times 157.6$  mm. Each detector can rotate a maximum of  $110^\circ$  without moving parts and is equipped with a square tungsten parallel-hole collimator (thickness: 0.2 mm, pitch: 2.46 mm, and length: 21.7 mm) [8, 15]. Data acquisition was completed in approximately two min in all of the phantom experiments. The collected data were reformatted (matrix size:  $64 \times 64$ , voxel size:  $4.92 \times 4.92 \times 4.92$  mm<sup>3</sup>) through reconstruction with a variant of

the ordered-subset expectation maximization (OSEM) algorithm and reorientation. A NaI-based A-SPECT system consists of dual-head rotating detectors that are equipped with a low-energy, parallel-hole, general-purpose (LEGP) collimator (thickness: 0.2 mm, pitch: 1.4 mm, and length: 24.7 mm). A set of 32 projection images was obtained (step-and-shoot method, 25 s/projection,  $64 \times 64$  matrices) over a  $90^\circ$  arc. Data acquisition was completed in approximately 15 min in all the phantom experiments. The collected data were reformatted (matrix size:  $64 \times 64$  and voxel size:  $6.39 \times 6.39 \times 6.39$  mm<sup>3</sup>) through reconstruction with a filtered back-projection and reorientation without attenuation correction.

### Evaluation of the CZT-SPECT System

The energy resolution and detector sensitivity were measured for Tc-99m (92.5 MBq), I-123 (92.5 MBq), and Tl-201 (92.5 MBq) using tube phantoms (inside diameter: 9.5 mm, height: 300 mm, and capacity: 21.3 mL) placed at the same locations. The energy and spatial resolutions were estimated from the calculation of full width at half maximum (FWHM) of the Gaussian curve obtained from each line source. In addition, we evaluated the energy resolution of the D-SPECT using a simultaneous dual-isotope (SDI) phantom with a solid defect in the myocardium region (RH-2, Kyoto-Kagaku, Japan). Tc-99m (44.0 MBq) and I-123 (22.0 MBq) were used to fill an SDI phantom. Tc-99m and I-123 data were simultaneously acquired in energy windows centered at 140 keV for Tc-99m and 159 keV for I-123 emission. The collected data were reformatted through reconstruction with a no-scatter correction (NSC) algorithm and reorientation. The spatial resolution was evaluated using a National Electrical Manufacturers Association (NEMA) phantom with three Tc-99m line sources (each source 1 mm in diameter with a length of 20 cm and radioactivity of 37 MBq) and reported as FWHM, in accordance with the relevant protocols and NEMA standards [16]. The measurement location of the rod is shown in Fig. 1. The MTF of the SPECT systems was performed by scanning a line source phantom (a Co-57 rod 1 mm in diameter with a height

**Fig. 1** Structure of the NEMA phantom and measurement location of the spatial resolution in the 3 Tc-99m line sources

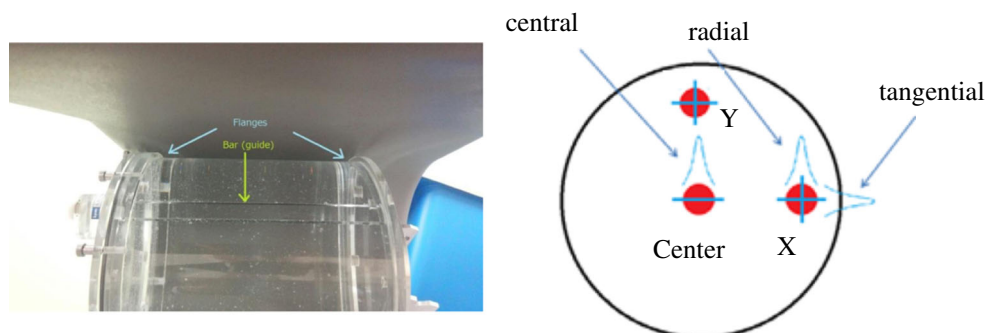
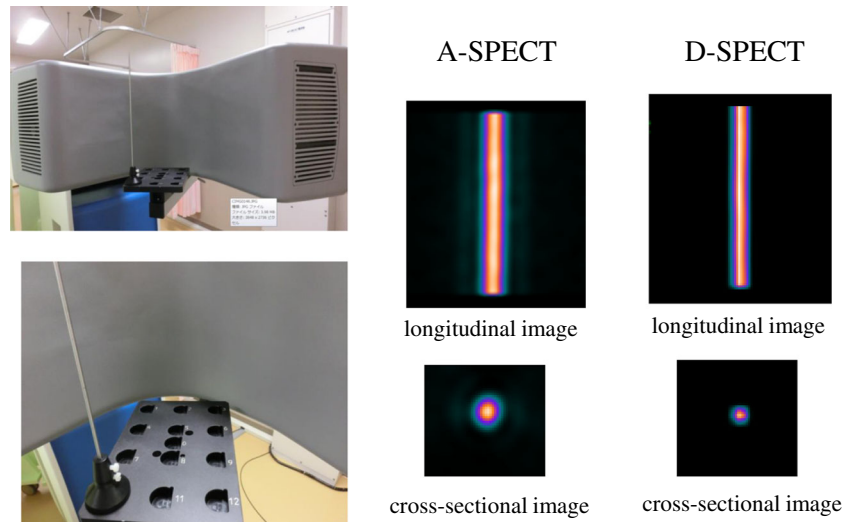


**Fig. 2** Acquisition image of D-SPECT and reconstruction images of a 1-mm-diameter Co-57 rod with both systems



of 180 mm and radioactivity of 370 MBq), which was measured by changing the CZT detector-line source distance to 8, 11, and 14 cm. The line spread function (LSF) was obtained by processing the scanned cross-sectional image of the Co-57 rod (Fig. 2). The MTF derived from the LSF was calculated using a one-dimensional fast Fourier transform [17, 18]. The geometric collimator resolution was calculated using the general method described by Anger [19]. The SPECT image of both systems was evaluated using the anthropomorphic torso phantom with a solid defect in the myocardium region (Data Spectrum Co, Hillsborough, NC, USA). Tl-201 (18.5 MBq) was used to fill a phantom. The OSEM algorithm was used for image reconfiguration and was chosen for the phantom experiment. In this study, two cardiologists and two radiological technologists participated in the phantom observation test.

### Evaluation of the A-SPECT System

The energy and spatial resolutions were in accordance with the NEMA standards. In addition, we evaluated the energy resolution using the same SDI phantom used in the D-

SPECT examination. The collected data were reformatted through reconstruction using filtered-back projection and reorientation with a no-scatter collection. The detector sensitivity was measured for Tc-99m, I-123, and Tl-201 using the same phantom used in the D-SPECT examination; these measurements were performed, if possible, at the same time. The corresponding measurement of the MTF was also performed for the A-SPECT system at a detector-line source distance of 12 cm. Corresponding measurements were performed using the same anthropomorphic torso phantom used in the D-SPECT examination.

### Results

Figure 3 shows the energy spectrum of the D-SPECT system at the (a) Tc-99m, (b) I-123, and (c) Tl-201 marker points, and Table 1 shows the FWHM of both systems. The energy resolution (FWHM) of the D-SPECT system with Tc-99m and I-123 was approximately two times higher than that of the A-SPECT system. Figure 4 shows

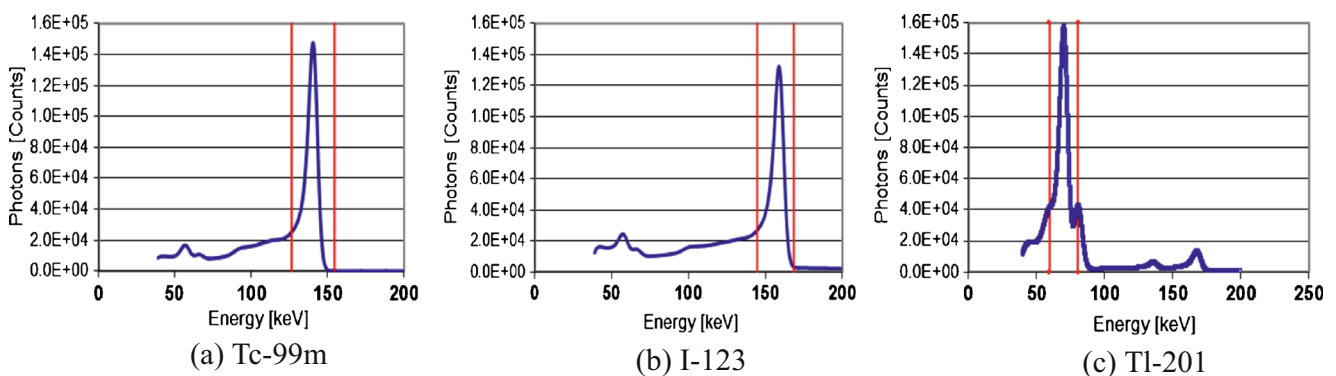


**Fig. 3** The energy spectrum of the D-SPECT system at **a** Tc-99m, **b** I-123, and **c** Tl-201. The red line shows the energy window width (20%)

**Table 1** The radionuclide energy resolutions (FWHM) measured from the energy spectrum of D-SPECT and A-SPECT

	Tc-99m	I-123	Tl-201
D-SPECT FWHM (%)	5.5	5.2	10.9
A-SPECT FWHM (%)	9.9	10.1	13.4

the short axis images of both systems on the SDI phantom with Tc-99m and I-123. The influence of cross-talk could not be detected by visual inspection by all observers on the D-SPECT images, unlike the A-SPECT images. Table 2 shows the radionuclide detector sensitivities of both systems. In the D-SPECT system, the Tc-99m, I-123, and Tl-201 markers showed detector sensitivities that were 4.2, 2.2, and 5.9 times higher than those of the A-SPECT system, respectively. Table 3 shows the results of the spatial resolution (FWHM) as measured using the NEMA phantom. The D-SPECT system had a spatial resolution (approximately two times higher than the average) superior to that of the A-SPECT system. Figure 5 shows the MTF of both systems, which was measured using the reconstructed image of the 1-mm Co-57 rod. The D-SPECT system had a superior MTF at all frequencies. However, the MTF obtained from the D-SPECT system was superior when the distance to the Co-57 rod was nearest to the CZT detectors (distance of 8 cm from the front). Figure 6 shows the calculated geometric resolution of the collimator according to the source-to-collimator distance. The collimator resolution (FWHM at a distance of 10 cm) of the A-SPECT system (7.6 mm) was superior to that of the D-SPECT system (13.3 mm). Figure 7 shows the images of both systems on the anthropomorphic torso phantom at Tl-201. In the visual inspection of the phantom images by all

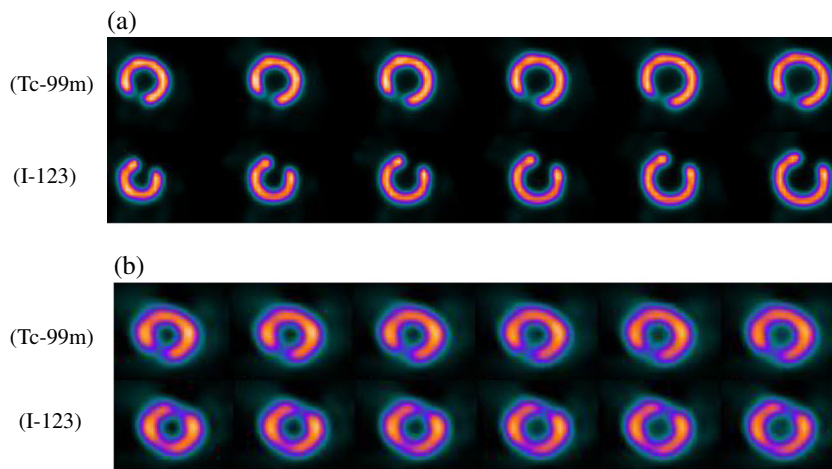
**Table 2** The radionuclide detector sensitivities of D-SPECT and A-SPECT

		Tc-99m	I-123	Tl-201
D-SPECT	Sensitivity (cpm/MBq)	34270	17973	56162
A-SPECT	Sensitivity (cpm/MBq)	8270	8000	9514
D-SPECT/A-SPECT		4.2	2.2	5.9

observers, the D-SPECT images clearly indicated better quality than the A-SPECT images and a well-defined myocardium defect.

## Discussion

We evaluated the performance of the CZT camera and collimation systems in the D-SPECT system in comparison with that of the conventional A-SPECT system in a clinical setting. We observed that D-SPECT could provide higher speed and resolution than the A-SPECT images, indicating better image qualities, and might reduce the radiation doses due to shortened acquisition times. Since 2009, many researchers have evaluated the performance of the D-SPECT system and compared it with the conventional A-SPECT systems [8–10]. However, because only the superior aspects of the D-SPECT system tend to be emphasized in reports, confirmation of the reliability of the system is necessary before introduction into clinical practice. For example, Gambhir et al. [8] reported that the D-SPECT system was “novel” and had “high sensitivity” and “high-energy resolution,” while, Erlandsson [9] and Verger et al. [10] reported similar opinions about A-SPECT. In addition to the same basic performance, we evaluated all types of tracers (Tc-99m, I-123, and Tl-201) that have been used in nuclear cardiology, the

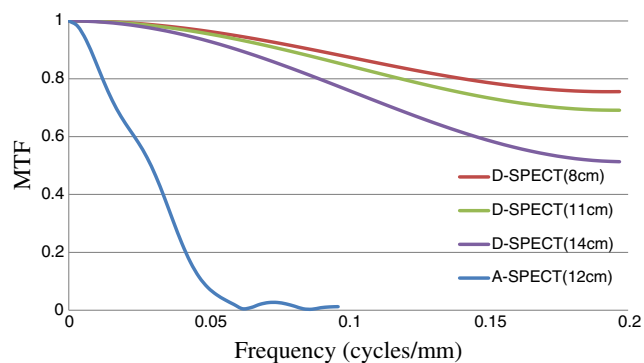
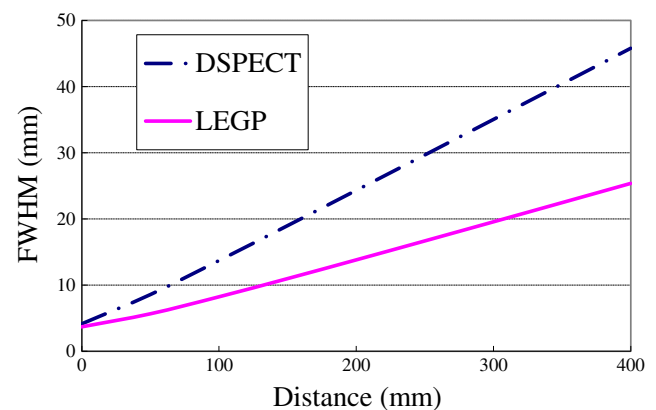
**Fig. 4** Comparison of the two systems based on SDI phantom images (short axis slices) with Tc-99m and I-123. **a** D-SPECT images. **b** A-SPECT images. For both systems, the upper panels depict Tc-99m images and the lower panels depict I-123 images

**Table 3** Spatial resolution (FWHM by three Tc-99m line sources) measured from the NEMA phantom images of D-SPECT and A-SPECT

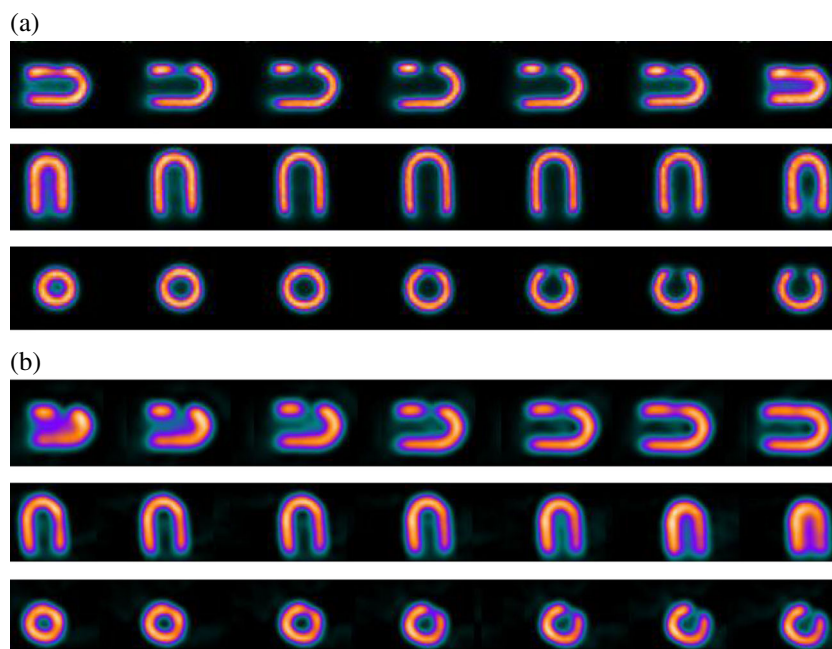
Measurement location of ROD Direction of measurement	X-FWHM (mm)		Y-FWHM (mm)		Center-FWHM (mm)
	Tangential	Radial	Tangential	Radial	Radial
	Mean (SD)	Mean (SD)	Mean (SD)	Mean (SD)	Mean (SD)
D-SPECT	2.89 (0.28)	4.67 (0.16)	4.37 (0.21)	2.61 (0.06)	6.90 (0.35)
A-SPECT	7.07 (0.17)	9.38 (0.22)	7.05 (0.25)	9.26 (0.35)	10.23 (0.31)

influences of the CZT detector-tracer distance on image quality using MTF, and the geometric collimator resolution using the general method described by Anger. This is the first report, to our knowledge, that evaluated the performances of the systems from the user's perspective. The Tc-99m and I-123 markers in the D-SPECT system showed an energy resolution that was approximately two times higher than that of the A-SPECT system. These results were expected considering the new possibility of dual-isotope SPECT imaging, such as the Tc-99m and I-123 combination, which provides low radiation doses and high patient throughput. We performed image reconstitutions with an NSC algorithm to confirm the influence of cross-talk with the use of simultaneous dual isotopes. The effect of cross-talk on simultaneous dual Tc-99m and I-123 SPECT imaging could not be detected by visual inspection of SDI phantom images. Tl-201 was slightly superior to the A-SPECT system in terms of FWHM (influence of a characteristic X-ray of Hg-201 in 20% of a window width of approximately 71 keV), but the energy resolution was set to approximately 5% in clinical practice, which was similar to that of Tc-99m and I-123 at the time of the collection. Gambhir et al. [8] reported that the sensitivity of the D-SPECT system was ten times greater than that of a conventional system equipped with a low-energy high-resolution collimator. However, our analyses, which focused on the sensitivity of an LEGP collimator (the most commonly used collimator in our practice) for myocardial tomography, found that the detector sensitivity was higher in the D-

SPECT system than in the A-SPECT system (Tc-99m: 4.2 times, I-123: 2.2 times, Tl-201: 5.9 times). Based on the detector sensitivity, thallium was thought to be suitable for the CZT camera. Nakazato et al. [20] reported that a 10 min stress scan could be performed with an effective average radiation dose of less than 1 mSv using the dedicated cardiac scanners. Our results might be associated with the reduction in radiation doses observed in clinical practice. The spatial resolution measured using a NEMA phantom was approximately two times higher on average than that of the A-SPECT system. In addition, the pixel size of the D-SPECT system was half that of the A-SPECT system, confirming the validity of these results. The MTF assessed using the D-SPECT system was superior to that assessed using the A-SPECT system for all frequencies. However, the MTF was affected by the CZT detector-line source distance. Specifically, a patient's body mass index (BMI) level at a detector-line source distance of 8, 11, and 14 cm, was approximately equivalent to 18, 20, and 37, respectively. These findings suggest potential problems with the body types and positioning of patients. In other words, stronger compression of the chest with the detector cover is an important step of the myocardium scan procedure. The geometric collimator resolution, which is an index of image quality, showed that the resolution of the D-SPECT system was 1.75 times lower than the A-SPECT system. Specifically, the resolution was lower because the tungsten

**Fig. 5** The MTFs of both systems that were measured on the reconstruction images of a 1-mm-diameter Co-57 rod. Each parenthesis (cm) indicates the distance from the detector**Fig. 6** The geometric resolution of the collimator that was calculated by using the source-to-collimator distance. The *dashed line* indicates the D-SPECT collimator, whereas the *solid line* indicates the A-SPECT collimator (LEGP)

**Fig. 7** Comparison of the two systems based on the anthropomorphic torso phantom images at TI-201. **a** D-SPECT images. **b** A-SPECT images



collimators used for the D-SPECT system have larger holes and shorter lengths than the lead parallel-hole collimators used for A-SPECT systems. However, each of the nine detectors is equipped with one collimator, hence the one-collimator resolution attached to the detector. Therefore, the overall collimator resolution of the D-SPECT system was not shown. Upon visual inspection, the D-SPECT system produced good-to-excellent image quality and better spatial resolution than the A-SPECT images. The myocardial edge was clear on the D-SPECT images; as a result, on first glance, the cardiac chambers appeared larger than their actual volumes. Claudin et al. [21] reported that the evaluation of left ventricular (LV) function using the D-SPECT system correlated well with that obtained using cardiac magnetic resonance imaging. However, LV volume depends on the cavity searching algorithm of quantitative perfusion SPECT or quantitative gated SPECT, which were developed based on A-SPECT [22]. Therefore, more studies need to be performed on this problem to validate the reliability of the D-SPECT system, including the factors that might influence the appearance of the myocardial edge and calculation of real volumes.

## Conclusion

The energy resolution, detector sensitivity, and spatial resolution of the D-SPECT system were superior to those of the conventional A-SPECT systems. The D-SPECT system shows good-to-excellent image quality and improved spatial resolution, and may significantly change the diagnostic process.

**Acknowledgements** The authors would like to acknowledge the assistance, support, and advice of the engineers of Spectrum Dynamics and the staff of Biosensors Japan. They also acknowledge the advice of Y. Banba and EIZO Corporation for the measurements of MTF.

## Compliance with Ethical Standards

**Conflict of Interest** Takanaga Niimi, Mamoru Nanasato, Mitsuo Sugimoto, and Hisatoshi Maeda declare that they have no conflict of interest associated with this study.

**Ethical Approval** The study was approved by an institutional review board and has been performed in accordance with the ethical standards laid down in the Helsinki Declaration of 1964 and later revision.

**Informed Consent** All subjects in the study gave written informed consent or the institutional review board waived the need to obtain informed consent.

## References

1. Berman DS, Germano G, Slomka PJ. Improvement in PET myocardial perfusion image quality and quantification with flurpiridaz F 18. *J Nucl Cardiol.* 2012;19 Suppl 1:S38–45.
2. Cutler SJ, Perez KL, Barnhart HX, Tornai MP. Observer detection limits for a dedicated SPECT breast imaging system. *Phys Med Biol.* 2010;55:1903–16.
3. Ogawa K, Ohmura N, Iida H, Nakamura K, Nakahara T, Kubo A. Development of an ultra-high resolution SPECT system with a CdTe semiconductor detector. *Ann Nucl Med.* 2009;23:763–70.
4. Lee CJ, Kupinski MA, Volokh L. Assessment of cardiac single-photon emission computed tomography performance using a scanning linear observer. *Med Phys.* 2013;40:011906.
5. Garcia EV, Faber TL, Esteves FP. Cardiac dedicated ultrafast SPECT cameras: new designs and clinical implications. *J Nucl Med.* 2011;52:210–7.

6. Neill J, Prvulovich EM, Fish MB, Berman DS, Slomka PJ, Sharir T, et al. Initial multicenter experience of high-speed myocardial perfusion imaging: comparison between high-speed and conventional single-photon emission computed tomography with angiographic validation. *Eur J Nucl Med Mol Imaging*. 2013;40:1084–94.
7. Duvall WL, Slomka PJ, Gerlach JR, Sweeny JM, Baber U, Croft LB, et al. High-efficiency SPECT MPI: comparison of automated quantification, visual interpretation, and coronary angiography. *J Nucl Cardiol*. 2013;20:763–73.
8. Gambhir SS, Berman DS, Ziffer J, Nagler M, Sandler M, Patton J, et al. A novel high-sensitivity rapid-acquisition single-photon cardiac imaging camera. *J Nucl Med*. 2009;50:635–43.
9. Erlandsson K, Kacperski K, van Gramberg D, Hutton BF. Performance evaluation of D-SPECT: a novel SPECT system for nuclear cardiology. *Phys Med Biol*. 2009;54:2635–49.
10. Verger A, Imbert L, Yagdigul Y, Fay R, Djaballah W, Rouzet F, et al. Factors affecting the myocardial activity acquired during exercise SPECT with a high-sensitivity cardiac CZT camera as compared with conventional Anger camera. *Eur J Nucl Med Mol Imaging*. 2014;41:522–8.
11. Zaman MU, Hashmi I, Fatima N. Recent developments and future prospects of SPECT myocardial perfusion imaging. *Ann Nucl Med*. 2010;24:565–9.
12. Nakazato R, Tamarappoo BK, Kang X, Wolak A, Kite F, Hayes SW, et al. Quantitative upright-supine high-speed SPECT myocardial perfusion imaging for detection of coronary artery disease: correlation with invasive coronary angiography. *J Nucl Med*. 2010;51:1724–31.
13. Hain SF, Van Gramberg D, Bomanji JB, Kayani I, Groves AM, Ben-Haim S. Can upright myocardial perfusion imaging be used alone with a solid-state dedicated cardiac camera? *Q J Nucl Med Mol Imaging*. 2013;57:383–90.
14. Ben-Haim S, Almukhailed O, Neill J, Slomka P, Allie R, Shiti D, et al. Clinical value of supine and upright myocardial perfusion imaging in obese patients using the D-SPECT camera. *J Nucl Cardiol*. 2014;21:478–85.
15. Park MA, Moore SC, Muller SP, McQuaid SJ, Kijewski MF. Performance of a high-sensitivity dedicated cardiac SPECT scanner for striatal uptake quantification in the brain based on analysis of projection data. *Med Phys*. 2013;40:042504.
16. NEMA Standards Publication. Performance measurements of gamma cameras. NU 1-2012. NEMA: Rosslyn, VA. 2013.
17. Hara T, Ichikawa K, Sanada S, Ida Y. Image quality dependence on in-plane positions and directions for MDCT images. *Eur J Radiol*. 2010;75:114–21.
18. Samartzis AP, Fountos GP, Kandarakis IS, Kounadi EP, Zoros EN, Skoura E, et al. A robust method, based on a novel source, for performance and diagnostic capabilities assessment of the positron emission tomography system. *Hell J Nucl Med*. 2014;17:97–105.
19. Anger HO. Scintillation camera with multichannel collimators. *J Nucl Med*. 1964;5:515–31.
20. Nakazato R, Berman DS, Hayes SW, Fish M, Padgett R, Xu Y, et al. Myocardial perfusion imaging with a solid-state camera: simulation of a very low dose imaging protocol. *J Nucl Med*. 2013;54:373–9.
21. Claudin M, Djaballah W, Imbert L, Veran N, Poussier S, Roch V, et al. Evaluation of left ventricular function using a semiconductor gamma camera and a fast low-dose protocol. *Med Nucl*. 2015;39:401–8.
22. Germano G, Kiat H, Kavanagh PB, Moriel M, Mazzanti M, Su HT, et al. Automatic quantification of ejection fraction from gated myocardial perfusion SPECT. *J Nucl Med*. 1995;36:2138–47.